จุฬาลงกรณ์มหาวิทยาลัย
ทุนวิจัย
กองทุนรัชดาภิเษกสมโภช

รายงานวิจัย

การเผาซินเทอร์ซิลิคอนไนไทรด์เซรามิกส์ในเตาอากาศ

โดย

สุพัตรา จินาวัฒน์
ปิยาภรณ์ ไชยพรรค
ชิเกทากะ วาดะ

พฤศจิกายน ๒๕๔๖

จุฬาลงกรณ์มหาวิทยาลัย

ทุนวิจัย

กองทุนรัชดาภิเษกสมโภช

รายงานผลการวิจัย

การเผาซินเทอร์ซิลิคอนไนไทรด์เซรามิกส์ในเตาอากาศ

โดย

ปิยาภรณ์ ไชยพรรค สุพัตรา จินาวัฒน์ และ ชิเกทากะ วาดะ

พฤศจิกายน 2546

Table of Contents

	Page
Abstract (Thai)	i
Abstract (English)	ii
Acknowledgements	iii
Chapter 1: Introduction	
Background	1
Introduction	1
Hypothesis	1
Objectives	2
Chapter 2: Experiment: Materials and methods	
2.1 Materials	3
2.1.1 Characteristics of starting materials	3
2.2 Methods	
2.2.1 Preparation of specimens	5
2.2.2 Temperature in the filler powder	8
2.2.3 Calculation of $SiO_{(g)}$ partial pressure	10
Chapter 3: Results and discussion	
3.1 Starting materials for specimens	12
3.2 Oxygen contents in the Si_3N_4 powders	15
3.3 Sintered specimens	16
Agglomeration of Al_2O_3 filler	17
Deterioration of Al_2O_3 crucible	17
Effect of packing powder on relative density and mass change	17
Mechanical properties of Si_3N_4 specimens	20
Chapter 4: Conclusion	24
Future suggestions	24
References	25
Appendices	
Appendix 1	26
Appendix 2	30
Appendix 3	32

List of Tables

	Page
Table 2.1 Physical and chemical properties of chemicals for test specimens	3
Table 2.2 Physical and chemical properties of Si_3N_4 packing powders	4
Table 2.3 Physical and chemical properties of Al_2O_3 fillers	4
Table 2.4 Sintering conditions for specimens of Si_3N_4, set A	9
Table 2.5 Sintering conditions for specimens of Si_3N_4, set B	9
Table 2.6 Calculated values of $P_{SiO(g)}$ and temperature	11
Table 3.1 Particle size analysis	12
Table 3.2 Oxygen contents in the powders	16
Table 3.3 Actual powder composition for Si_3N_4 specimens, set A	16
Table 3.4 Actual powder composition for Si_3N_4 specimens, set B	16
Table 3.5 Mass change of SN-F2 packing powder	19
Table 3.6 Hv and K_{1C} of specimens	20
Table A-1a Mass change, bulk and relative densities of specimens, Set A	26
Table A-1b Mass change, bulk and relative densities of specimens, Set B	27
Table A-1c Alpha content in sintered specimens, Set A	27
Table A-1d Alpha content in sintered specimens, Set B	28
Table A-2a Results of fracture toughness and Vickers hardness of sintered specimens at 1700°C, measured by SEM	30
Table A-2b Results of fracture toughness and Vickers hardness of sintered specimens at 1700°C, measured by OM	30
Table A-2c Calculated results of biaxial bending strength	31

List of Figures

	Page
Fig. 2.1 Flow chart of the experiment	6
Fig. 2.2 Arrangement of specimens under sintering	7
Fig. 2.3 Relation between the temperatures in the furnace	8
Fig. 2.4 Relation between $P_{SiO(g)}$ and temperature	10
Fig 3.1 Particle size distributions of powders, Set A	12
Fig. 3.2 Particle size distributions of powders, Set, B	13
Fig. 3.3 Cumulative wt% coarse than of SN-F2	14
Fig. 3.4 Photographs of the packing powders after sintering of sopecimens, Set B	15
Fig. 3.5 Bulk densities of sintered specimens, Set A	18
Fig. 3.6 Bulk densities of sintered specimens, Set B	18
Fig. 3.7 Mass change of Si_3N_4 specimens, Set A	19
Fig. 3.8 Mass change of Si_3N_4 specimens, Set B	19
Fig. 3.9 Indents of Si_3N_4 specimens	20
Fig. 3.10 Schematic diagram of cracks	20
Fig. 3.11 Weibull plots of bending strengths at 25°C	21
Fig. 3.12 a- contents of sintered specimens, Set B	21
Fig. 3.13 SEM micrographs of a fractured specimen, Set B	22
Fig. 3.14 SEM micrographs of polished and plasma etched specimen, Set B	23
Fig. A-1 Example of XRD patterns of specimens and packing powders	29

ชื่อโครงการ การเผาซินเทอร์ซิลิคอนไนไทรด์เซรามิกส์ในเตาอากาศ

ผู้วิจัย ปิยาภรณ์ ไชยพรรค สุพัตรา จินาวัฒน์ ชิเกทากะ วาดะ

เดือนและปีที่ทำวิจัยเสร็จ พฤศจิกายน 2546

บทคัดย่อ

การเผาซินเทอร์ซิลิคอนไนไทรด์เซรามิกส์ในเตาอากาศ

ชิ้นตัวอย่างเซรามิกส์ที่เตรียมจากการอัดผงแอลฟ่า-ซิลิคอนไนไทรด์ผสมสารเติมแต่งอิทเทรียและอลูมินา ได้ถูกเผาซินเทอร์ ที่อุณหภูมิ 1550-1700 องศาเซลเซียสในอากาศเป็นผลสำเร็จโดยไม่มีการสูญหายของมวลมากนัก โดยใช้อลูมินาครูซิเบิลชนิดที่มีความบริสุทธิ์สูงซึ่งออกแบบมาเป็นพิเศษ ภายในบรรจุผงซิลิคอนไนไทรด์และอลูมินา พบว่าขณะเผาเกิดการจับตัวเป็นก้อนของผงที่บรรจุทั้งสองชนิด แต่สามารถจะควบคุมได้โดยเลือกใช้ผงที่มีขนาดใหญ่ขึ้น นอกจากนี้ครูซิเบิลถูกกัดกร่อนหลังจากใช้งานสองสามครั้ง จึงยังต้องมีการปรับปรุงในเรื่องของความทนทาน อย่างไรก็ตามสามารถเผาซินเทอร์ซิลิคอนไนไทรด์เซรามิกส์ให้มีความหนาแน่นสูงสุด(98%) ได้ที่อุณหภูมิ 1700 องศาเซลเซียส ในเวลา 2 ชั่วโมง โดยมีค่าความแข็งแรงดัดชนิดไบแอกเชี่ยลเฉลี่ย เท่ากับ 420 เมกะปาสคาล ค่าความแข็งวิคเกอร์เท่ากับ16 กิกกะปาสคาล และ ค่าแฟรคเจอทัฟเนส เท่ากับ 5 เมกะปาสคาลเมตร$^{1/2}$

คำสำคัญ: ซิลิคอนไนไตรด์เซรามิกส์ การเผาซินเตอร์ในอากาศ ครูซิเบิล การเปลี่ยนแปลงมวล

Project Title: Sintering of Si_3N_4 ceramics in an air atmosphere furnace
Name of the Investigators: Piyaporn Chaiyapuck, Supatra Jinawath and Shigetaka Wada
Year: October 2003

Abstract

Sintering of Si_3N_4 ceramics in an air atmosphere furnace

Pressed specimens of α-Si_3N_4 (SN-E10) powder with Y_2O_3 and Al_2O_3 additives were successfully sintered without a serious mass loss at a temperature range of 1550-1700°C in an air atmosphere furnace using a set of specially designed, high purity Al_2O_3 crucibles, Si_3N_4 packing powder and Al_2O_3 filler. The agglomeration on sintering of both the packing powder and Al_2O_3 filler was encountered, but it could be optimized by using coarse size materials. Additionally, the deterioration of Al_2O_3 crucibles leading to cracking after several times of usage is still to be improved. On the contrary, Si_3N_4 ceramics could be sintered to full density (98%) reproducibly at 1700°C for 2 hours with an average biaxial bending strength of 420 MPa, Vickers hardness of 16 GPa and fracture toughness, K_{1C}, of 5 $MPam^{1/2}$.

Keywords: Si_3N_4 ceramics, sintering in air atmosphere, crucible, mass change

Acknowledgements

The authors gratefully thank the Rachadapiseksomphot Endowment, Chulalongkorn University, for the financial support. The help in characterization of the specimens from Mr. Thanakorn Wasanapienpong and the collaborative facilities at the Department of Geology, Faculty of Science, the Scientific and Technological Research Equipment Center, Chulalongkorn University and The Siam Research and Development Co. Ltd. are sincerely acknowledged.

Chapter 1

Introduction

Background:

Both α-Si_3N_4 and β-Si_3N_4 have hexagonal structure but difference in the sequence of Si-N layer stacking. This results in different unit cell structures. β-Si_3N_4 is columnar grain with a half c-axis of α-Si_3N_4. α-Si_3N_4 is equiaxed grain with twice the c-axis of β-Si_3N_4. β-Si_3N_4 is a more stable form (high temperature form) and has higher theoretical density (3.19 g/cm^3) than α-Si_3N_4 (3.16 g/cm^3), hence it has a better mechanical strength. However, the composite of the 2 phases is quite common. Normally dense β-Si_3N_4 bodies are sintered from α-rich starting powder (containing 3-7 vol%β-Si_3N_4). Due to the high covalent nature (~75%) of the Si-N bond, Si_3N_4 is difficult to densify without the help of sinteing aids, i.e. Y_2O_3, MgO, CeO_2. They are added to react with surface SiO_2 of the Si_3N_4 powder and form a grain boundary glassy phase. These phenomena assist rearrangement of particles to achieve densification. During liquid phase sintering, $\alpha \rightarrow \beta$-Si_3N_4 phase transformation taking place, and in addition, it is believed that α-Si_3N_4 also dissolves in the glassy phase and precipitates as rod-like β-Si_3N_4, hence grain growth occurs. This is known as solution precipitation mechanism.

Introduction:

Si_3N_4 is a very important high strength, high temperature ceramic. Its utilization is extensive, e.g. as parts in diesel engines, which would be operative at temperature above the useful range for super alloys and energy transfer devices. Due to the passive oxidation of Si_3N_4 to SiO_2, commercial Si_3N_4 ceramics are sintered in pressurized N_2 atmosphere. However, nitrogen furnaces consume nitrogen gas and need much amount of water for cooling. Decreasing the production cost has been expected to increase the utilization of Si_3N_4 ceramics. For low-cost fabrication of Si_3N_4 ceramics, non-pressurized sintering in N_2 gas may be a feasible production method. Wada et al. reported, first in the world, a method to sinter Si_3N_4 ceramics in an air furnace based on the basic researches on mass loss reactions of Si_3N_4 ceramics during sintering (1-3). However, the reports only showed possibility of sintering Si_3N_4 in an air furnace. More experiments are essential to complete the findings. To establish and verify competitiveness in properties and excellence in production cost of Si_3N_4 ceramics sintered in an air furnace compared to those sintered in a N_2 furnace is very important and challenging from the stand point of practical applications of the technology in industry.

Hypothesis:

According to Wada et al., Si_3N_4 ceramics undergo a mass loss through the following reactions:

In N_2 atmosphere

$$Si_3N_4(s) + 3SiO_2(l) = 6SiO(g) + 2N_2(g) \quad (1)$$

In air atmosphere

$$Si_3N_4(s) + 3O_2(g) = 3SiO_2(l) + 2N_2(g) \quad (2)$$, passive oxidation,

$PO_2 \sim 2 \times 10^4$ Pa

$2Si_3N_4(s) + 3O_2(g) = 6SiO(g) + 4N_2(g)$ (3), active oxidation,

1650-1700°C $PO_2<1 \times 10^2$ Pa

Reaction (1) is responsible to the major mass loss of Si_3N_4 during sintering. When specimen is packed in Si_3N_4 powder, the $P_{SiO(g)}$ can be kept high to oppose the mass loss of specimen. This reaction also can accelerate the change of the reaction from (2) to (3). In air atmosphere, Reaction (2) takes part in the early stage of sintering and later when the pressure of O_2 drops, reaction (3) dominates. Moreover the pressure of O_2 around Si_3N_4 specimens can be kept low when using a specially designed Al_2O_3 sagger and Si_3N_4 or Si_3N_4-SiO_2 powder beds. Hence Si_3N_4 ceramics can be sintered without serious mass loss in air atmosphere.

Objective:

The objective is to experimentally demonstrate that Si_3N_4 ceramics can be sintered in an air furnace by

1. Establishing the method to sinter silicon nitride (Si_3N_4) ceramics in air furnace,
2. Studying the properties of the obtained silicon nitride in comparison with the commercial.

Chapter 2

Experiment

Materials and methods

2.1 Materials:

Si_3N_4 powder (SN-E10, Ube Ind., Ltd., Japan)
Y_2O_3 powder (RU, Shin-Etsu Chemical Co., Ltd., Japan)
Al_2O_3 powder (AKP-30, Taimei Chemical Co., Ltd., Japan)
Al_2O_3 filler: AM-21 (Sumitomo Chemicals) and A-11 (Fuji Kasei Co., Ltd.)
Si_3N_4 packing powders: SN-7, SN-F2 (Denki Kagaku Kogyo Co., Ltd.) and SN-K05, SN-E10 (Ube Ind., Ltd.)
Al_2O_3 crucibles (Nikkato SSA-S, 50 and 150 cm^3, O.D. 80 x I.D. 68 x 23 H and O.D.102 x I.D. 105 x 34.5 H cm^3)
h-BN packing powder (Denki Kagaku Kogyo Co., Ltd.), BN = 99.9 wt%
O.D. = outer diameter, I.D. = inner diameter

2.1.1 Characteristics of starting materials

Table 2.1 Physical and chemical properties of chemicals for test specimens (from suppliers and experiment,Table 3.1)

Type	Si_3N_4 (SN-E10)	Y_2O_3	Al_2O_3 (AKP-30)
Alpha-phase, wt %	>95		
	Fe < 100 ppm	Y_2O_3 99.99	Al_2O_3 99.99
	Al trace	SiO_2 0.0087	
	Ca trace	Fe_2O_3 0.001	
	O < 2.0 wt%	Al_2O_3 0.001	
	Cl < 100 ppm	CaO 0.0007	
*Specific surface area (m^2/g)	9-13 (10.45)	29.9	
**Mean particle size,μm	0.83		
***Tap density, g/cm^3	0.63		

* BET method, ** sedimentation method, *** Tap-Pak volumeter method

Table 2.2 Physical and chemical properties of S_3N_4 packing powders (from suppliers and experiment)

Type	SN-7	SN-K05	SN-F2
Alpha-phase, wt%	74.0	81.6	<1
Chemical composition	Si 59 wt% N 38 wt% Fe 0.3 Al 0.2 Ca 0.2 Mg < 0.1 O 1.6	 N 38 wt% Fe ≤300 ppm Al ≤500 ppm Ca ≤100 ppm Cl ≤100 ppm O 0.62 wt% (reference value)	Free Si <0.5 wt% - Fe 0.2 wt% Al 0.1wt% Ca 0.1 wt5 Cl < 100 ppm O < 2.0 wt%
Specific Surface area, m^2/g	4 (3.79)	4-6 (5.03)	1 (0.89)
Mean particle size μm	3.40	1.68	2.22 (fine) 21.71(coarse)
Tap density, g/cm^3	1.16	0.68	1.61(fine) 1.39(coarse)

Table 2.3 Physical and chemical properties of Al_2O_3 fillers (from suppliers and experiment)

Qualitative data/grade		A-11	AM-21
Chemical composition	LOI , wt%	0.01	0.05
	Fe_2O_3	0.01	0.01
	SiO_2	0.01	0.02
	Na_2O	0.30	0.26
	Al_2O_3	99.7	99.7
	H_2O	0.06	0.10
Physical composition	True specific gravity	3.93	3.95
	Apparent specific gravity		
	Packed bulk density,g/cm^3	-	1.3
	Loose bulk density	-	0.70
	Mean particle size, μm	9.0	4.0
	Specific surface area, m^2/g	0.79	1.27
	Tap density, g/cm^3	0.96	1.67

2.2 Methods:

2.2.1 Preparation of specimens:

Two sets of specimens were prepared, Set A; 92 wt% of Si_3N_4 (E10) : 3 wt% of Al_2O_3(AKP-30) : 5 wt% of Y_2O_3 and Set B; 90 wt% of Si_3N_4 (E10) : 5 wt% of Al_2O_3(AKP-30) : 5 wt% of Y_2O_3. About 40 g of A and B mixtures were each ground in a Si_3N_4 ball mill (500 ml), using Si_3N_4 media balls and absolute ethanol as medium for 24 and 192 h, respectively. The content was dried at 80°C, sieved through a 100 mesh screen. Then the powder was compacted into pellet of 25 mm diameter x 5 mm thickness by a hydraulic press at 20 MPa and followed by a cold isostatic press (CIP) at 200 MPa. The obtained specimens were placed in the small Al_2O_3 crucible, embedded with Si_3N_4 packing powder. Then the covered crucible was set in the bigger one and covered with Al_2O_3 filler up to the top, and sintered in air at temperatures of 1550-1700°C. After sintering, the specimens were characterized for bulk density by Archimedes' method, phase analysis by XRD (D8-Advance, Bruker, Ltd.), cross section morphology by SEM (JSM-5410 LV, JEOL Co.,Ltd.), hardness by Vickers indentation (Zwick 3212, Rank Taylor Hobson, Ltd.) and biaxial bending strength in conformity to ASTM F-394 (LLOYD 500), respectively. The flow chart of experiment is presented in Fig. 2.1 and the experimental conditions are tabulated in Table 2.1-2.3. The arrangement of the specimens under sintering in the high purity and specially designed crucibles with packing powder and filler to hinder the oxidation of the specimens from the atmospheric oxygen is in Fig. 2.2. The relation between the temperatures in the furnace, outside the crucible and inside the filler, is shown in Fig 2.3.

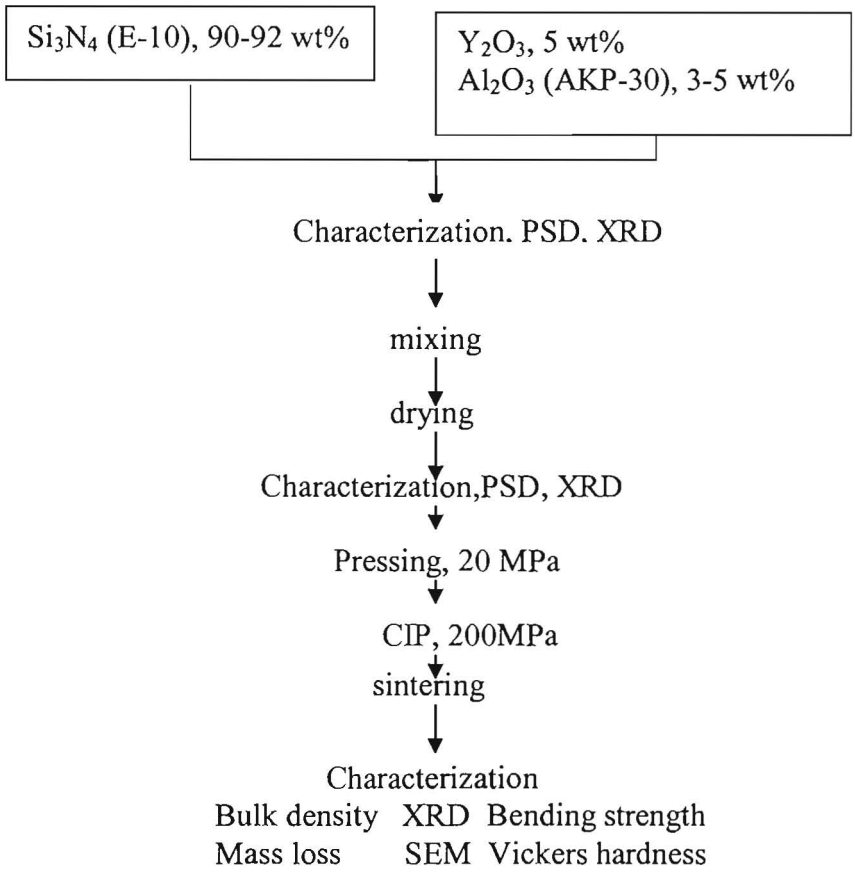

Fig. 2.1 Flowchart of the experiment

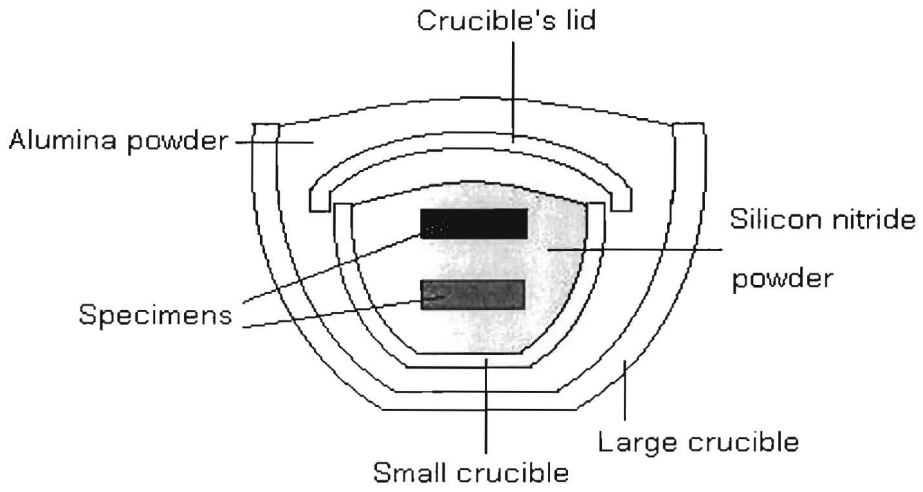

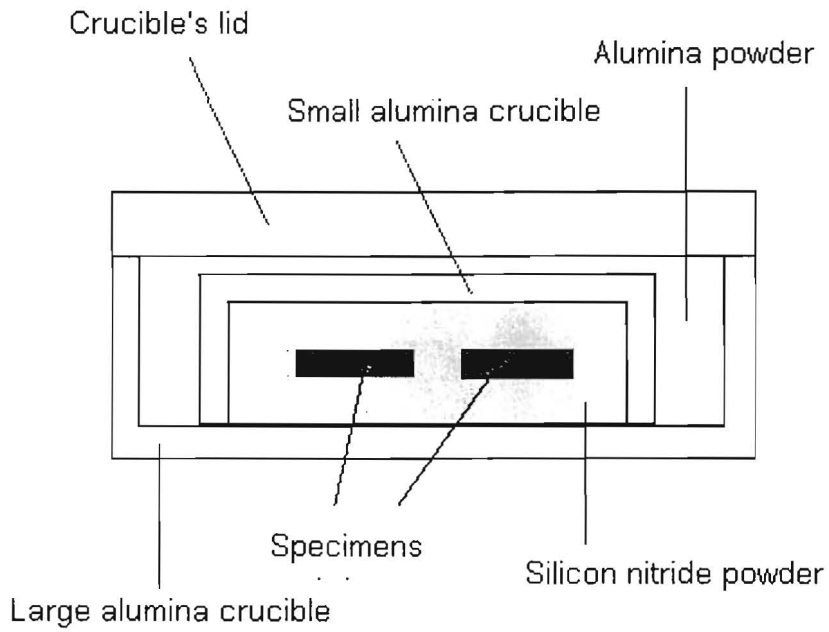

Fig. 2.2 Arrangement of specimens under sintering

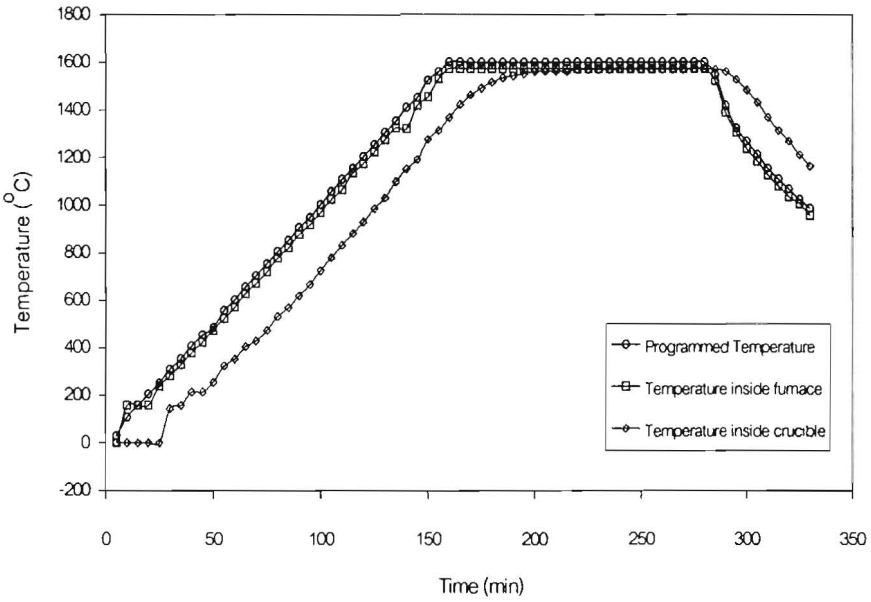

Fig. 2.3 Relation between the temperatures in the furnace, inside the furnace and inside the crucible (filler)

2.2.2 Temperature in the filler powder:

It was presumed that the temperature of the specimen was the same as that of the filler and should be less than that of the furnace therefore a blank run with an R-type thermocouple setting in the center of the large crucible filled with Al_2O_3 filler was performed at a constant heating rate of 10°C/min. The results plotted in Fig.2.3 show that the temperature of the filler always lags about 200°C behind and reaches the soaking temperature after 30 min of the onset. However, the delay may not be so serious when we consider the difference in mind.

Table 2.4 Sintering conditions for specimens of Si_3N_4, Set A

Specimen A, no.	Temperature °C	Packing powders	Heating rate °C /min	Cooling rate °C /min	Soaking time,h
C1	1550	SN-7,AM-21	5	5	2
C2	1550	SN-E-10,AM-21	5	5	2
C3	1550	(SN-7+BN),A11	5	5	2
C4	1550	SN-E10,A11	5	5	2
C5	1600	(SN-7+BN),A11	5	5	2
C6	1600	SN-E10,A11	5	5	2
C7	1600	(SN-7+BN),A11	5	5	2
C8	1600	SN-E10,A11	10	Natural	2
C9	1650	(SN-7+BN),A11	10	Natural	2
C10	1650	SN-E10,A11	10	Natural	2
C11	1700	(SN-7+BN),A11	10	Natural	1
C12	1700	SN-E10,A11	10	Natural	1
C13	1700	SN-E10,A11	10	Natural	2

10 wt% BN was added to hinder the agglomeration of SN-7.
Natural cooling: leaving the specimens cool down to room temperature after switching off at the end of the firing program.
Furnace atmosphere: air

Table 2.5 Sintering conditions of specimens of Si_3N_4, Set B

Specimen B, no.	Temperature,°C	Packing powders	Heating Rate,°C/min	Cooling Rate, °C/min	Soaking Time,h
E1	1650	Lot1 SN-K05,A11	10	Natural	2
E2	1650	Lot1 SN-F2,A11	10	Natural	2
E3	1700	Lot1 SN-K05,A11	10	Natural	1
E4	1700	Lot2 SN-K05,A11	10	Natural	1
E5	1700	Lot1 SN-F2,A11	10	Natural	1
E6	1700	Lot2 SN-F2,A11	10	Natural	1
E7	1700	Lot1 SN-K05,A11	10	Natural	2
E8	1700	Lot2 SN-K05,A11	10	Natural	2
E9	1700	Lot1 SN-F2,A11	10	Natural	2
E10	1700	Lot2 SN-F2,A11	10	Natural	2

2.2.3 Calculation of $SiO_{(g)}$ partial pressure, $P_{sio(g)}$, of the system

According to Wada, $P_{SiO(g)}$ is responsible to the loss of mass by oxidation during sintering of Si_3N_4. However, under a controlled condition, $P_{SiO(g)}$ may oppose to the diffusion of O_2 from air and if $P_{SiO(g)}$ can be kept high throughout the course of sintering, the active reaction becomes dominant and the oxidation of Si_3N_4 will be greatly hindered. Therefore, the relation between $P_{SiO(g)}$ and sintering temperature, based on the following reaction, has to be known.

$$Si3N4(s) + 3\ SiO2\ (l) \quad = \quad 6\ SiO(g) + 2\ N2(g)$$

The equilibrium value of $P_{SiO(g)}$ at any temperature can be calculated using equation of mass action expression

$$\Delta G = \Delta G^{o} + RT \ln K$$

Where

K, equilibrium constant of the reaction, = $(P_{SiO(g)})^{6}.(P_{N2})^{2}$

P_{N2} is taken as 0.8 atm (based on the volume ratio of O_2/N_2 = 21/79 at room temperature under 1 atm). R, gas constant, = 1.9872×10^{3} $Kcal.mol^{-1}.K^{-1}$.

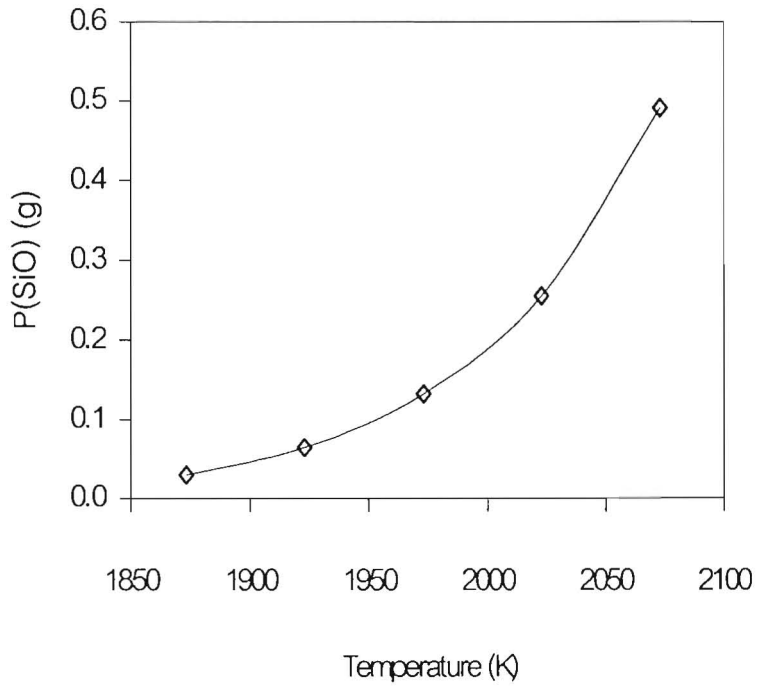

Fig. 2.4 Relationship between $P_{SiO(g)}$ and temperature

Table 2.6 Calculated values of $P_{SiO(g)}$ at temperatures 1873-2073 K

$Si_3N_4(s)+ 3SiO_2(l) = 6SiO(g) + 4N_2(g)$					$P_{SiO(g)}$ atm
T/ ΔGo	$Si_3N_4(s)$	$SiO_2(l)$	SiO(g)	$N_2(g)$	
1873	-26.922	-137.571	-59.935	0	0.030
1923	-22.054	-135.262	-60.491	0	0.064
1973	-16.807	-132.961	-61.043	0	0.132
2023	-12.347	-130.666	-61.593	0	0.255
2073	-7.124	-128.376	-62.139	0	0.491

ΔGo in kcal/mole

Chapter 3

Results and discussion

3.1 Starting materials for specimens Set A and B:

Average particle sizes of all the employed powders are presented in Table 3.1, and their particle size distributions are shown in Fig. 3.1-3.2.

Table 3.1 Particle size analysis

powder	Average particle size μm
A, 24 h milling	0.69
B,192 h milling	0.61
SN-E10	0.83
SN-7	3.40
SN-K05	1.68
AM-21	2.87
A-11	9.02
Fine SN-F2	2.22
Coarse SN-F2	21.71

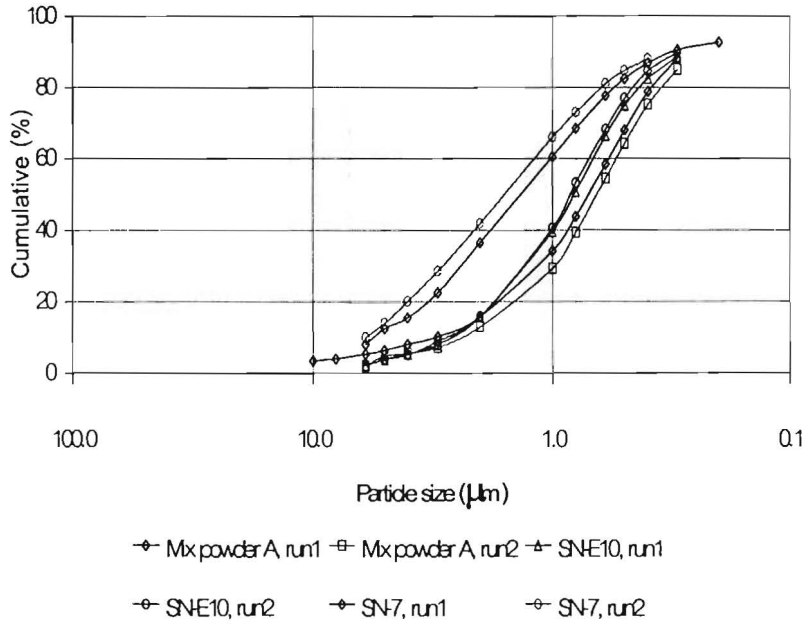

Fig 3.1 Particle size distributions of powders, Set A, SN-E10 and SN-7

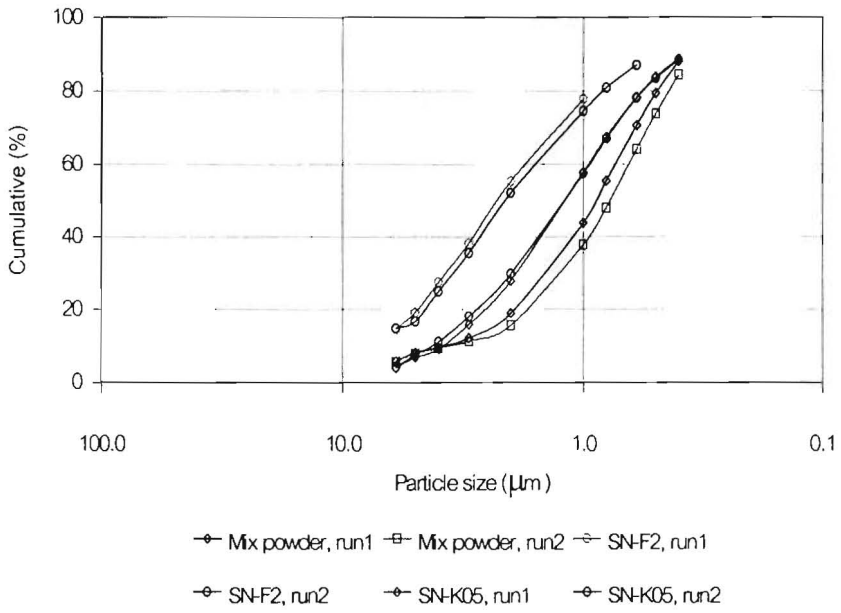

Fig. 3.2 Particle size distributions of powders, Set B, SN-K05 and SN-F2

The results of particle size analysis show that, despite the longer milling time, the average particle size of powder B is not much different from that of A. However, they are much smaller than those of the packing powders of which SN-F2 is the largest.

Being the cheapest, packing powder SN-F2 was chosen for further sintering experiment The good packing powders must be inert to chemical reaction and can ensure an adequate $P_{SiO(g)}$ in the system, and must also be quite resistant to glass forming resulted from oxidation. Melting glass will lead to agglomeration on cooling, hence resulting in difficulty in taking out the imbedded specimen. In this matter, the purity and size of the packing powder are critical. Therefore, the size of SN-F2 was classified into fractions by dry sieve method as presented in Fig. 3.3, and fractions of fine size, -45 μm, and coarse size, -300 +75 μm (Table 3.1) were chosen for the study together with the other packing powders. After sintering, the extents of agglomeration of all the packing powders mentioned in Tables 2.2-2.4 are observed and presented in Fig. 3.4.

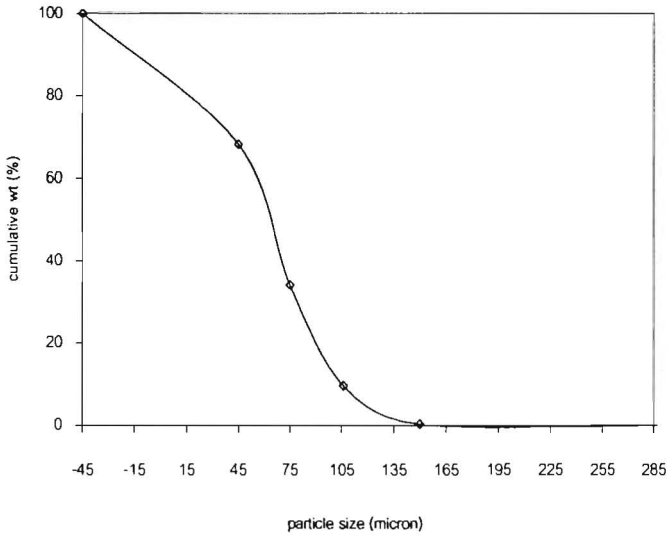

Fig. 3.3 Cumulative wt% coarser than of SN-F2

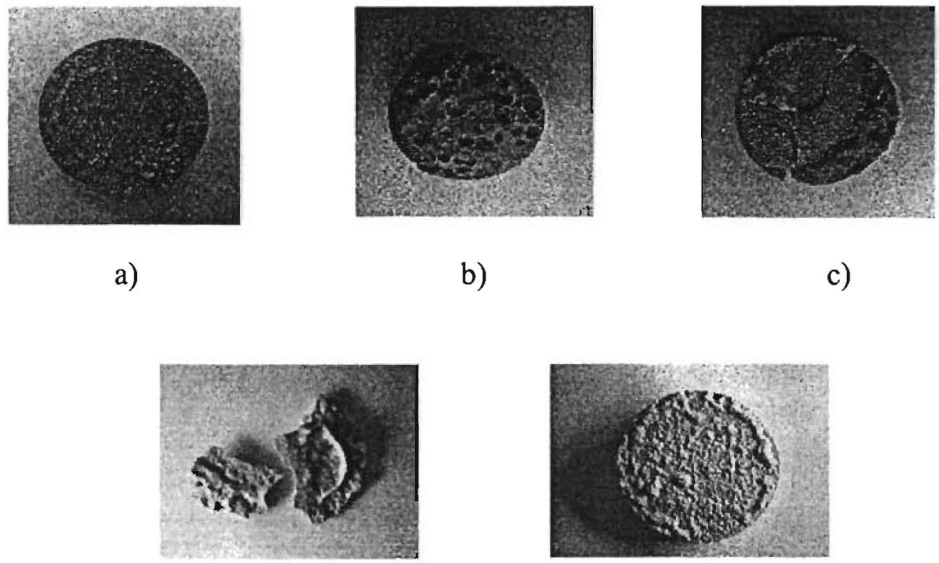

a) b) c)

d) e)

Fig. 3.4 Photographs of the packing powders after sintering of specimens, Set B
a) SN-7 + BN, 1550°C, 2h at a heating rate of 5°C/min
b) SN-7 + BN, 1600°C, 2h at a heating rate of 5°C/min
c) SN-7 + BN, 1600°C, 2h at a heating rate of 10°C/min
d) SN-F2, 1700°C, 1 h at a heating rate of 10°C/min
e) SN-F2, 1700°C, 2 h at a heating rate of 10°C/min

SN-7+BN packing powder showed less agglomeration than SN-7 after sintering of specimens Set A at 1550°C but at higher temperatures (1600-1700°C), extensive glass layer formed on the surface of the packing bed due to the lower melting point of B_2O_3 which came from the oxidation of BN, and A-11 showed loose agglomeration. Due to their lower cost, SN-K05, SN-F2 and A-11 were used as packing powders in the sintering of specimens set B at 1650-1700°C. They all showed the same result, i.e. cracking of the packing bed at low temperatures and formation of thin layer of glass at 1700°C but only sparing agglomeration appeared in the case of +75 μm SN-F2. Besides the purity and size of the packing powders, the fast heating rate could also reduce the extent of oxidation.

3.2 Oxygen contents in the Si_3N_4 powders:

O content in the employed powders, both for the specimens and for packing, is very important because it is a measure of the extent of oxidation before sintering, and is directly related to the oxidation product, SiO_2. The sources of O_2 are mostly from the decomposition of the ethanol used as milling medium and sparingly from the atmosphere.

O contents in the powders employed were determined by chemical analysis performed by the Siam Research and Development Co., Ltd. The results are presented in Table 3.2.

Table 3.2 Oxygen contents in the powders

Powder	Oxygen, wt% O
B, 192 h milling	7.06
A, 24 h milling	4.42
SN-F2 packing powder	1.18

Based on the assumption that, under the normal condition (room temperature and 1 atm), Si_3N_4 contains about 1 wt% of O_2 as contamination[4], and the theoretical densities of Si_3N_4, SiO_2, Y_2O_3 and Al_2O_3 are 3.22, 2.2, 4.84 and 4.0 g/cm3, respectively, the O contents in each green powder before milling are calculated. Those after milling are also calculated based on the determined values taken from Table 3.2. They are shown in Table 3.3 and 3.4, respectively. It is found that the increase in O content[5] of powder B after milling is higher than that of powder A.

Table 3.3 Actual powder composition for Si_3N_4 specimens, Set A

powder	Formulated composition	Before milling, wt%		After milling, wt%	
		O content	Actual	O content	actual
Si_3N_4	92	-	90.27	-	88.34
SiO_2	-	0.92	1.73	1.95	3.66
Y_2O_3	5	1.06	5	1.06	5
Al_2O_3	3	1.41	3	1.41	3
Total	100	3.39	100	4.42	100

Table 3.4 Actual powder composition for Si_3N_4 specimens, Set B

Powder	Formulated composition	Before milling, wt%		After milling, wt%	
		O content	Actual	O content	Actual
Si_3N_4	90	-	88.31	-	83.14
SiO_2	-	0.9	1.69	3.65	6.90
Y_2O_3	5	1.06	5	1.06	5
Al_2O_3	5	2.35	5	2.35	5
Total	100	4.31	100	7.06	100

3.3 Sintered specimens:

Agglomeration of Si_3N_4 packing powder: The phenomena relating to packing powder after sintering are agglomeration, formation of surface layer and sticking of the lid to the body of the crucible. The degree of agglomeration depended on the sintering temperature and type of packing powder, i.e. purity, packing density (expressed as tap density) and particle size. Fig.3.4 shows the results of agglomeration. Low purity and fine SN-7 packing powder (high tap density) agglomerated strongly even at 1550°C while higher purity and finer E-10 and SN K-05 did not agglomerate so much even at 1700°C. Coarse packing powder, SN-F2, strongly agglomerated at over 1650°C but the large size SN-F2, prepared by selectively sieving the as-

purchased (Fig. 3.3), slightly did. The tap densities are presented in Table 2.1, 2.2 and 2.3, and their effect on the agglomeration, in Fig. 3.4.

Agglomeration of Al_2O_3 filler: Without the Al_2O_3 filler in between the two crucibles, Si_3N_4 packing powder formed a thick block-like scrap under the lid. Therefore, Al_2O_3 filler was essential in the crucible setting. The degree of agglomeration of the Al_2O_3 filler also depended on sintering temperature and type of the Al_2O_3 as follows: AM-21>AW-100>A-11. After sintering at 1700°C for 2 h, A-11 could be de-agglomerated by hand and reused for several times. The data in Table 2.3 suggested coarse particle size and low tap density be the two important factors in suppressing the agglomeration of the Al_2O_3 filler.

Deterioration of Al_2O_3 crucible: The large crucible cracked after 7-8 times of usage at 1700°C. This might come from the thermal stress induced by the high heating rate (10 °C/min) employed. After usage, the color of the inner wall of the small crucible changed from white to grey and some bubbles were generated at over 1650°C. It also cracked after 3-4 reuses but, coating with Al_2O_3 slurry, the service could be extended to >5 times. However, it was estimated to be less than 10 times at 1700°C. XRD analysis suggested the formation of silicon oxy-nitride ($Si_{12}Al_{18}O_{39}N_8$), by the following reactions:

$$6SiO_2(s) + 2Si_3N_4(s) + 9Al_2O_3(s) = Si_{12}Al_{18}O_{39}N_8(s) \quad (1)$$

$$12SiO(g) + 9Al2O3(s) + 4N2(g) = Si_{12}Al_{18}O_{39}N_8(s) \quad (2)$$

Since all the substances in reaction (1) were solid and the Si_3N_4 powder was loosely packed in the small crucible, high activation energy was required to initiate the reaction. Then reaction (1) was difficult to occur.

Effect of packing powder on relative density and mass change: Relative densities of powder Set A (Fig.3.5) increased with temperature, but did not reach full density at 1700°C. Surprisingly, the density and mass change were also affected by the type of packing powder (Table 3.5). The mass change, expressed as %wt loss, was mostly negative (Fig. 3.5 and 3.6) when using packing powder, E-10, but was mostly positive in the case of SN-7. Totally, the mass change went from positive to negative with increasing temperature. On the contrary, relative densities of powder, Set B (Fig. 3.7), reached almost full density at 1650°C. The relative densities of specimens sintered in SN-F2 packing powder was a little higher than those in SN-K05 and their mass change also went further into the negative side. The trend of mass change with temperature (Fig. 3.8 and 3.9) can be explained as follows: The mass gain (positive) is thought to be due to the oxidation of Si_3N_4[6] during heating up. The mass loss (negative) comes from the reaction between Si_3N_4 and SiO_2[7], and increases with temperature because the SiO(g) partial pressure becomes high with increasing temperature[8].The mass loss reaction is affected by the ease of the SiO(g) diffusion through the packing powder and filler. When hard surface layer was formed in the case of SN-7, the diffusion of SiO(g) might be disturbed. As a result, mass changes were slightly positive. However, the reason why the relative density was affected by the type of packing powder in this experiment, can not be clarified. The rest of the experimental data on density and mass change are tabulated in Appendix 1.

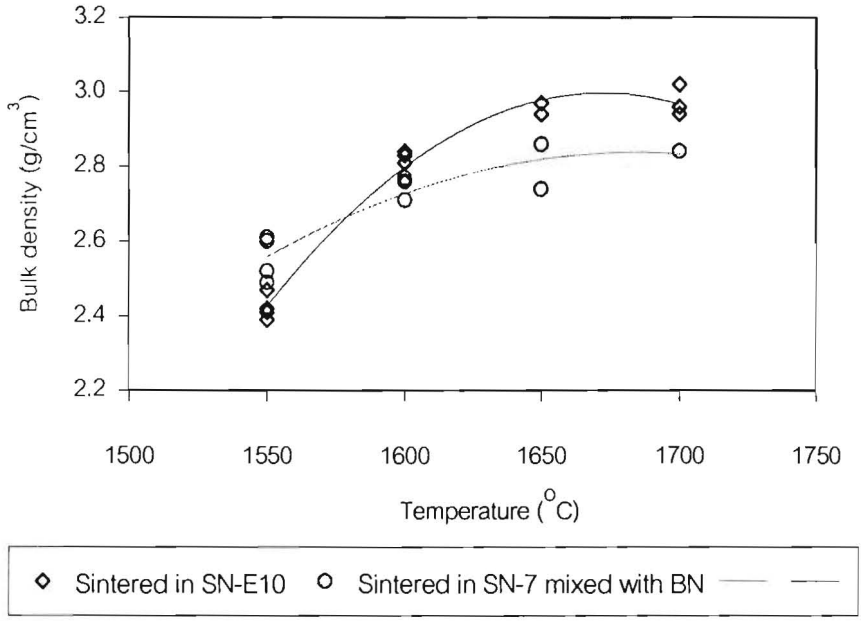

Fig.3.5 Bulk densities of sintered specimens, Set A at various temperatures

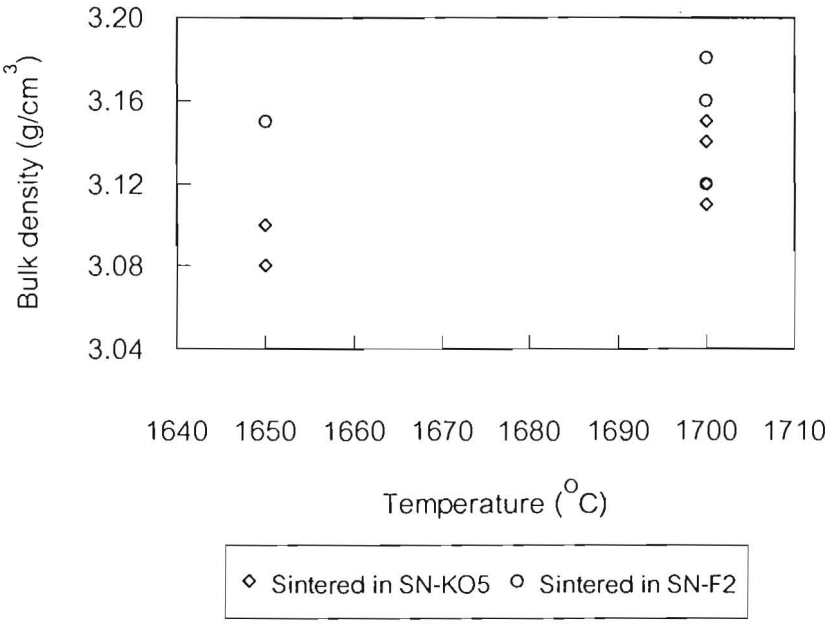

Fig. 3.6 Bulk densities of Si_3N_4 specimens sintered in various packing powders

Table 3.5 Mass change of SN-F2 packing powder at 1650°C

Packing powder	Sample No.	Mass change, wt% Coarse	Fine
SN-F2	1	-0.78	-0.96
	2	-0.67	-0.94

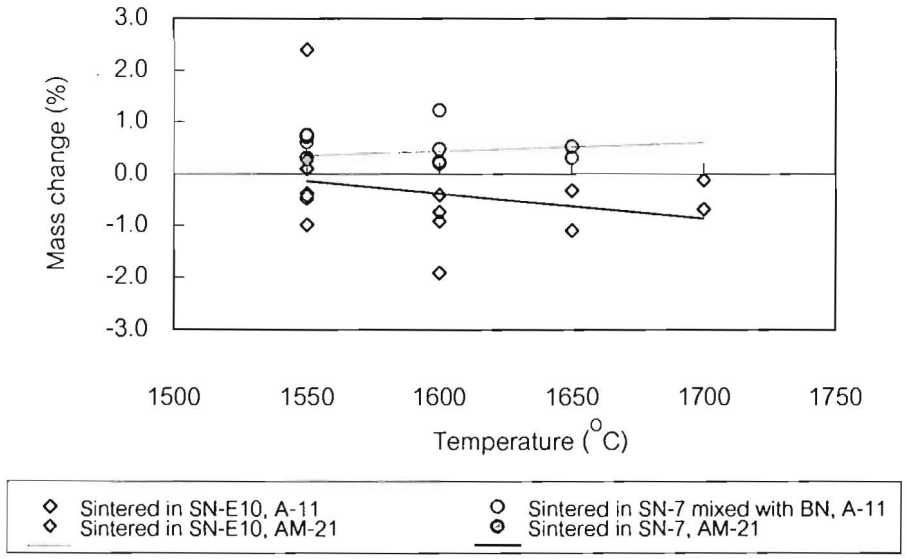

Fig. 3.7 Mass change of Si_3N_4 specimens, Set A, sintered in various packing powders

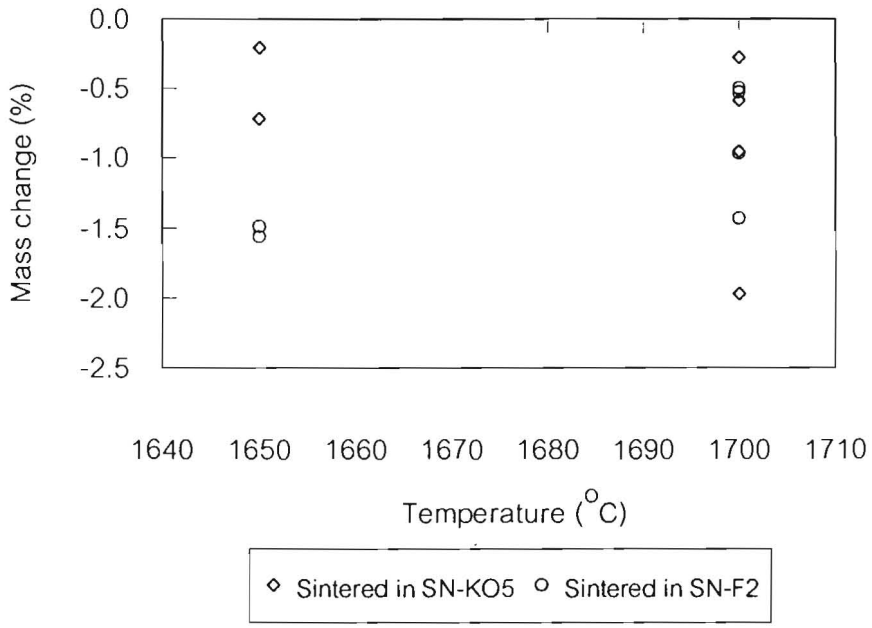

Fig.3.8 Mass change of Si_3N_4 specimens, Set B, sintered in various packing powders

Mechanical properties of Si3N4 specimens:

Vickers hardness, fracture toughness, and biaxial bending strength of the sintered specimens at 1700°C for 2 h are presented in Table 3.6 (additional details are included in Appendix 2 and 3). Although the values of Vickers hardness and fracture toughness are compatible with the commercial product (Toshiba, Appendix 3), the value of mechanical strength is not high enough. The rather low biaxial bending strength value comes from the residual α-Si_3N_4 (Fig. 3.12). The grain sizes of α-Si_3N_4 and β-Si_3N_4 shown in the SEM microstructure, Fig. 3.13 and 3.14, are smaller than 1 μm while that of Si_2N_2O is about 5 μm. However, better details of the grains are shown in Fig. 3.15 and 3.16.

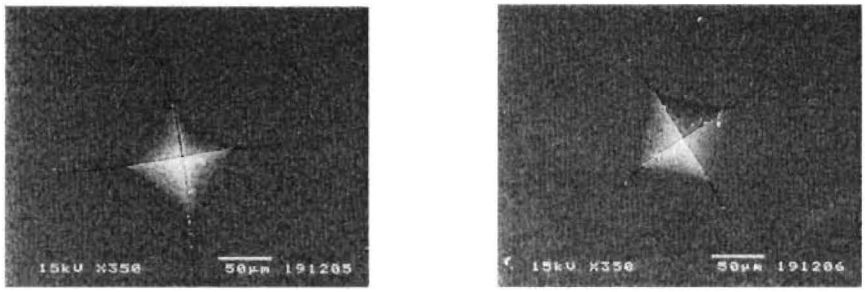

Fig. 3.9 Indents of Si_3N_4 specimens sintered at 1700°C
(a) 1 h soaking, (b) 2 h soaking

Table 3.6 Hv and K_{1C} of specimens sintered at 1700°C for 1 and 2 h

Soaking Time, h	K_{1C}(MPa.m$^{1/2}$) SEM	Microscope	Hv(GPa) SEM	Microscope	α-content wt%	Bulk Density, g/cm^3
1	4.7	5.2	17.4	16.6	39	3.16
2	5.0	5.1	15.9	15.7	18	3.18

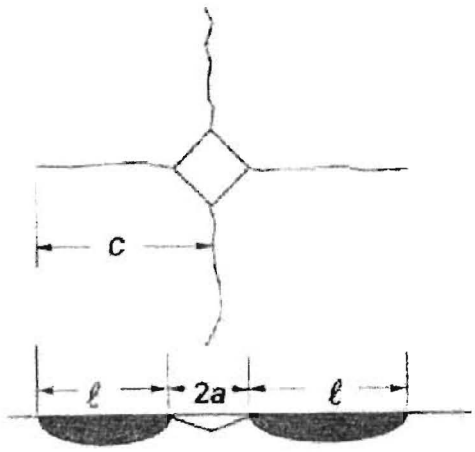

Fig. 3.10 Schematic diagram of cracks

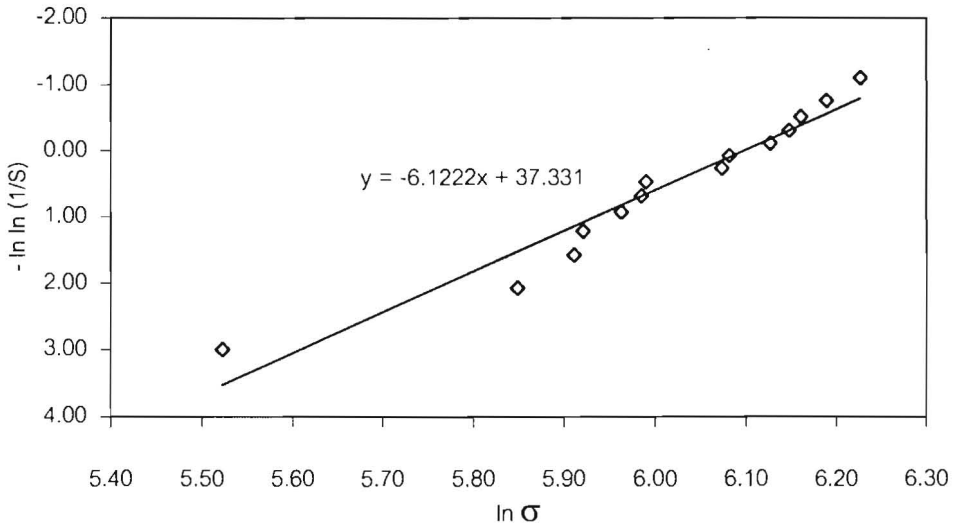

Fig. 3.11 Weibull plots of bending strengths at 25°C

Fig. 3.19 and 3.10 are the examples of SEM micrographs of the indents and their schematic diagram used in the calculation of K_{1C}, respectively. Fig 3.11 is the curve of Weibull plot[9] of bending strengths of sintered specimens according to the experimental data and equations given in Appendix 2.

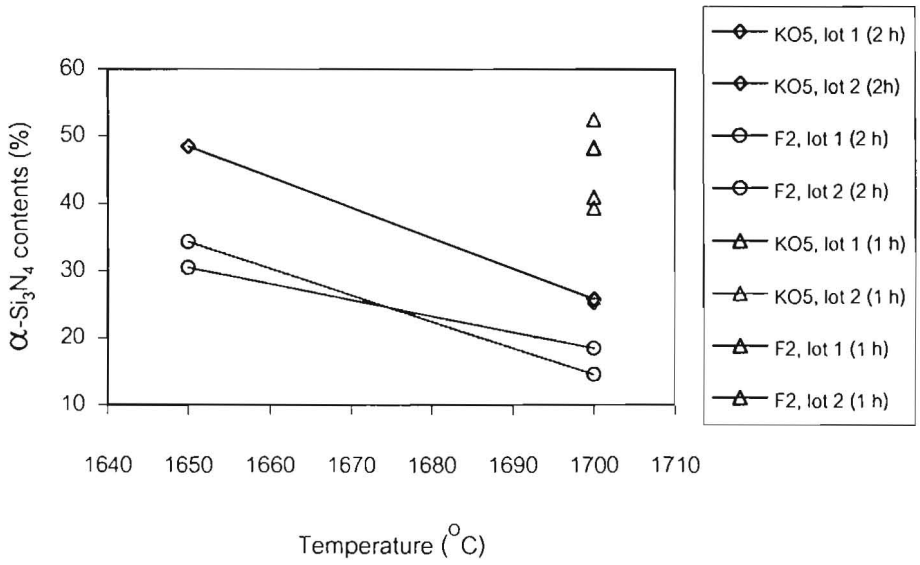

Fig. 3.12 α-Si_3N_4 contents of sintered specimens, Set B

The α-Si_3N_4 contents of sintered specimens were calculated from the relative intensity between the α-Si_3N_4 and β-Si_3N_4 peaks in the XRD patterns (Appendix 1,Table A-1c and A-1d) as suggested by Gazzara and Messier[10].

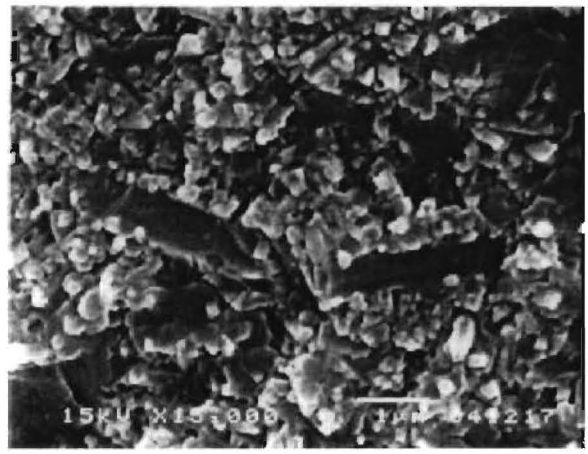

(a)

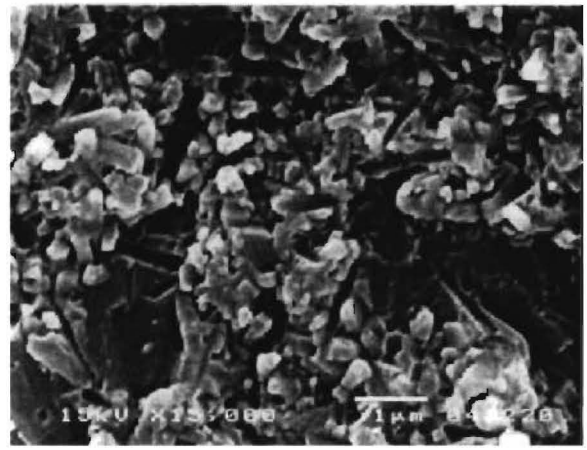

(b)

Fig. 3.13 SEM micrographs of a fractured specimen, Set B (Lot 2), sintered at 1700°C with SN-F2 packing powder. (a) 1 h soaking, (b) 2 h soaking.

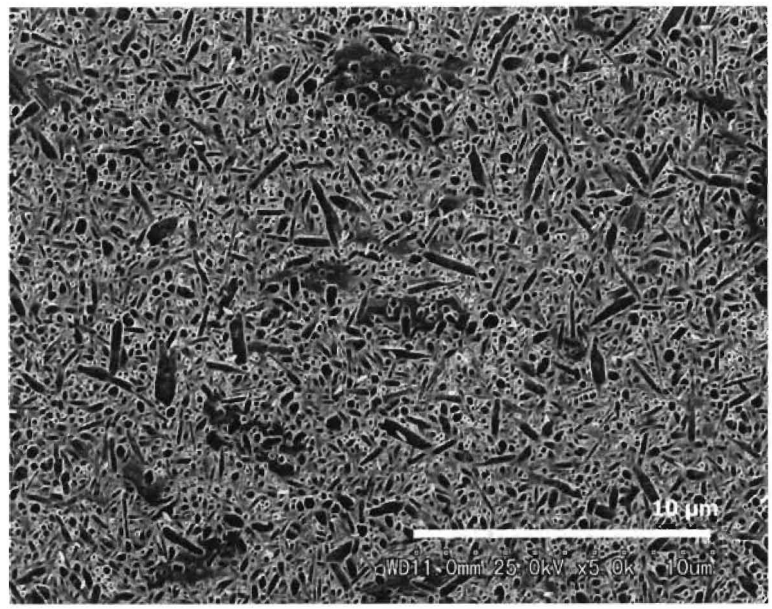

(a)

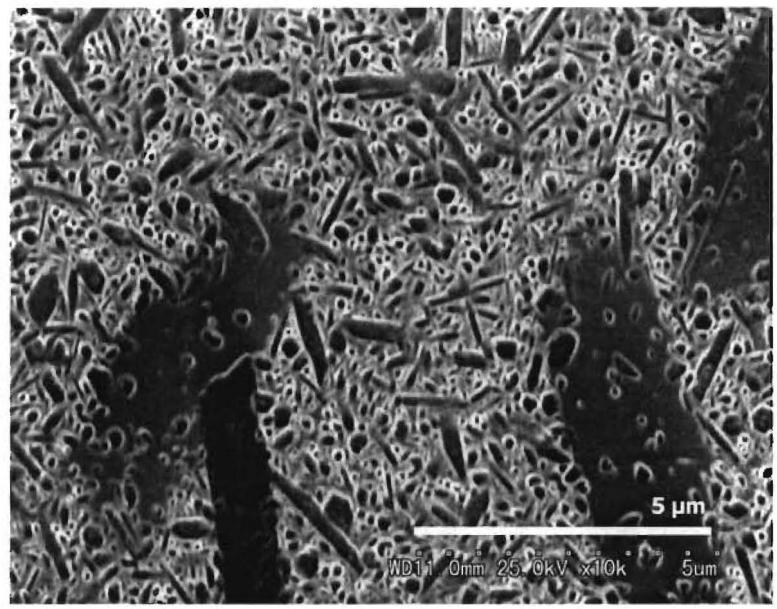

(b)

Fig. 3.14 SEM micrographs of polished and plasma etched specimen, Set B, sintered at 1700° with SN-F2 packing powder (1h soaking).

Analysing by XRD, the sintered specimens are composed of α-Si_3N_4, β-Si_3N_4 S_2N_2O and small amout of unknown phase. Revealing by SEM (Fig. 3.14), both α-Si_3N_4 (equiaxial grain) and β-Si_3N_4 (elongated or needle-like grain) grains are very small, < 0.5 μm and the length of β-Si_3N_4 is ~ 1 μm. Grains showing abnormal growth are thought to be S_2N_2O, about 1-2 μm in diameter and 10 μm in length.

Chapter 4

Conclusion

Si_3N_4 ceramic could be sintered to almost full density without serious oxidation and mass loss in air atmosphere furnace using alumina crucible, Si_3N_4 packing powder and Al_2O_3 filler. Considering the process cost, SN-F2 was the best candidate for packing powder and Al_2O_3 powder larger than 1 μm did not agglomerate seriously even at 1700°C. On the contrary, Al_2O_3 crucible filled with Si_3N_4 packing powder deteriorated and cracked after only several usages. The specimens sintered at 1700°C for 2 h had the values of Vickers hardness and fracture toughness of about 16 GPa and 5 MPa.$m^{1/2}$, respectively, which were compatible with those of commercial product but their mechanical strength (420 MPa) was rather low due to residual α-Si_3N_4 from the incomplete $\alpha \rightarrow \beta$ transformation. However, with these properties, they may be used as media balls, cutting tools and wear-resistant applications.

Future suggestions:

Some more experiments should be carried out on the followings:

1. Improvement of the mechanical strength: by raising sintering temperature slightly beyond 1700°C which is at present the limitation of our furnace.
2. Improvement of the deterioration of the Al_2O_3 crucible: by finding a better material for crucible, for example mullite crucibles.
3. Improvement of the grinding and mixing methods to reduce the content of glass phase (SiO_2), for example by applying vacuum to get rid of any O_2 occurring during these processes.

References

1. Wada, S., Hattori, T. and Yokoyama, K., J. Ceram. Soc. Japan, 109, 281-83 (2001).
2. Wada, S., J. Ceram. Soc. Japan, 109, 803-08 (2001).
3. Wada, S., Material Integration, 14 (7), 7-11 (2001) (in Japanese).
4. Wada, S., Kondo, Y., Sudo, E., and Maki, Y., J. Ceram. Soc. Japan, 107, 611-14 (1999).
5. Wada, S., J. Ceram. Soc. Japan, 104, 1085-87 (1996).
6. Yokoyama, K., and Wada, S., J. Ceram. Soc. Japan, 108, 627-32 (2000).
7. Yokoyama, K., and Wada, S., J. Ceram. Soc. Japan, 108, 357-64 (2000).
8. Hattori, T., and Wada, S., J. Ceram. Soc. Japan, 109, 960-62 (2001).
9. Basoum, M.W. Fundamentals of ceramics. International Editions.Singapore: McGraw-Hill Companies Inc., 1997.
10. Gazzara, C.P.and Messier, D.R., J. Am. Ceram. Soc., 56, 777-80 (1977).

APPENDIX 1

Table A-1a Mass change, Bulk and relative densities of sintered specimens,Set A

	Conditions					Sample No.	Mass change (%)	Bulk density (%)	Relative density (%)
	T °C	Rate °C/min	Soaking h	Packing powders					
				Si_3N_4	Al_2O_3				
C1	1550	5	2	SN-7 BN	AM-21	1 2	0.71 0.75	2.49 2.52	75.91 76.73
C2	1550	5	2	SN-E10	AM-21	1 2	-0.43 0.27	2.41 2.39	73.47 72.73
C3	1550	5	2	SN-7 BN	A-11	1 2	-0.46 0.31	2.60 2.61	79.28 79.68
C4	1550	5	2	SN-E10	A-11	1 2	0.10 2.40	2.42 2.47	73.89 75.19
C5	1600	5	2	SN-7 BN	A-11	1 2	0.61 0.75	2.76 2.77	84.28 84.44
C6	1600	5	2	SN-E10	A-11	1 2	-0.99 -0.38	2.81 2.76	85.56 84.15
C7	1600	10	2	SN-7 BN	A-11	1 2	0.20 1.23	2.71 2.71	82.62 82.53
C8	1600	10	2	SN-E10	A-11	1 2	-0.92 -0.41	2.83 2.84	86.18 86.50
C9	1650	10	2	SN-7 BN	A-11	1 2	0.24 0.48	2.86 2.74	86.59 83.54
C10	1650	10	2	SN-E10	A-11	1 2	-0.74 -1.91	2.94 2.97	89.63 90.55
C11	1700	10	1	SN-7 BN	A-11	1 2	0.31 0.53	2.84 2.84	86.59 86.59
C12	1700	10	1	SN-E10	A-11	1 2	-0.32 -1.09	2.94 2.96	89.63 90.24
C13	1700	10	2	SN-E10	A-11	1 2	-0.12 -0.68	2.96 3.02	90.24 92.07

Table A-1b Mass change, Bulk and relative densities of sintered specimens, Set B

	Conditions					Lot No.	Mass change (%)	Bulk density (%)	Relative density (%)
	T ^{o}C	Rate ^{o}C/min	Soaking h	Packing powders Si_3N_4	Al_2O_3				
E1	1650	10	2	SN-KO5	A-11	1 2	-0.20 -0.72	3.10 3.08	95.09 94.48
E2	1650	10	2	SN-F2	A-11	1 2	-1.56 -1.49	3.15 3.15	96.63 96.63
E3	1700	10	2	SN-KO5	A-11	1	-0.59	3.11	95.40
E4	1700	10	2	SN-F2	A-11	1	-0.52	3.12	95.71
E5	1700	10	2	SN-KO5	A-11	2	-0.28	3.12	95.71
E6	1700	10	2	SN-F2	A-11	2	-0.96	3.16	96.93
E7	1700	10	2	SN-KO5	A-11	1	-1.97	3.14	93.32
E8	1700	10	2	SN-F2	A-11	1	-1.44	3.16	93.93
E9	1700	10	2	SN-KO5	A-11	2	-0.95	3.15	96.93

Table A-1c Alpha content (%) in sintered specimens, Set A

Temperature (^{O}C)	Alpha content (%) SN-7+ 10 wt % BN		Alpha content (%) SN-E10	
	5 ^{O}C/min	10 ^{O}C/min	5 ^{O}C/min	10 ^{O}C/min
1550, 2 h	20.9	-	94.9	-
1550, 2 h	-	92.4	-	78.3
1600, 2 h	48.9	-	82.2	-
1600, 2 h	-	60.6	-	71.8
1650, 2 h	-	21.6	-	48.3
1700, 1 h	-	30.1	-	34.9
1700, 2 h	-	-	-	20.9

Table A-1d Alpha content (%) in sintered specimens, Set B

Temperature (^{O}C)	Alpha Content (%) SN-KO5		Alpha Content (%) SN-F2	
	Lot 1	Lot 2	Lot 1	Lot 2
1650, 2 h (10^{O}C/min)	48.5	-	34.3	30.5
1700, 1 h (10^{O}C/min)	48.2	52.4	40.9	39.3
1700, 2 h (10^{O}C/min)	25.8	25.2	14.5	18.5

α-Si_3N_4 content was calculated from the XRD pattern using the intensities of 7 peaks of α-Si_3N_4 and 4 peaks of β-Si_3N_4 as suggested by Gazzara and Messier[10]. Fig. A-1 is the examples of the XRD patterns of sintered Si_3N_4.

Light blue = Si_2ON_2
Blue = α-Si_3N_4
Red = β-Si_3N_4

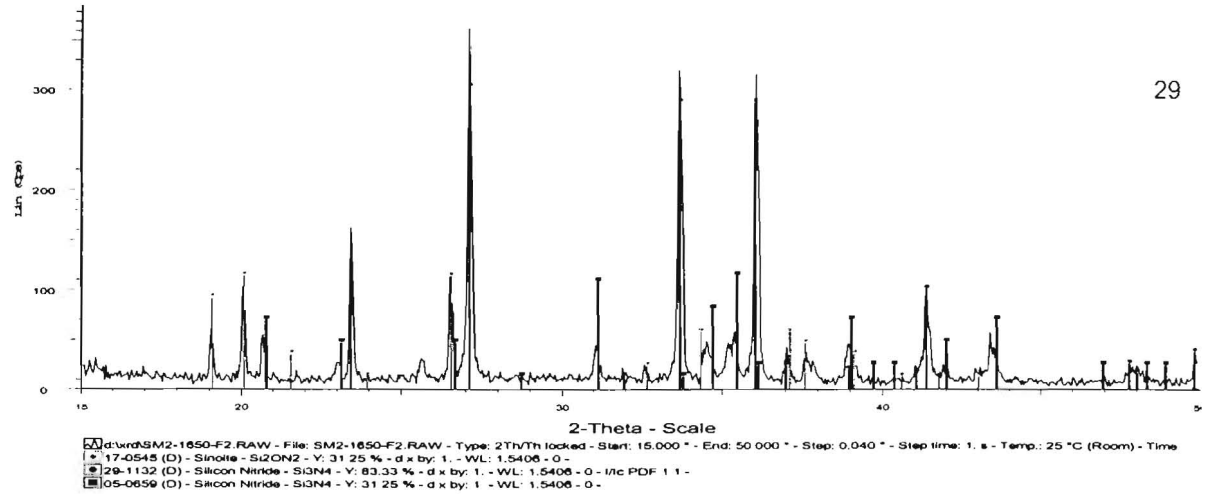

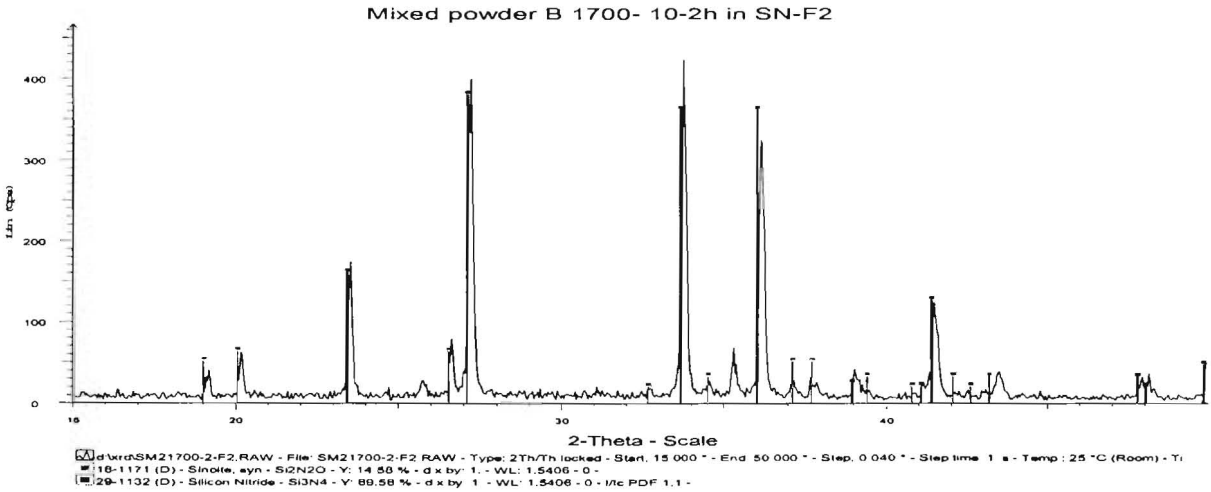

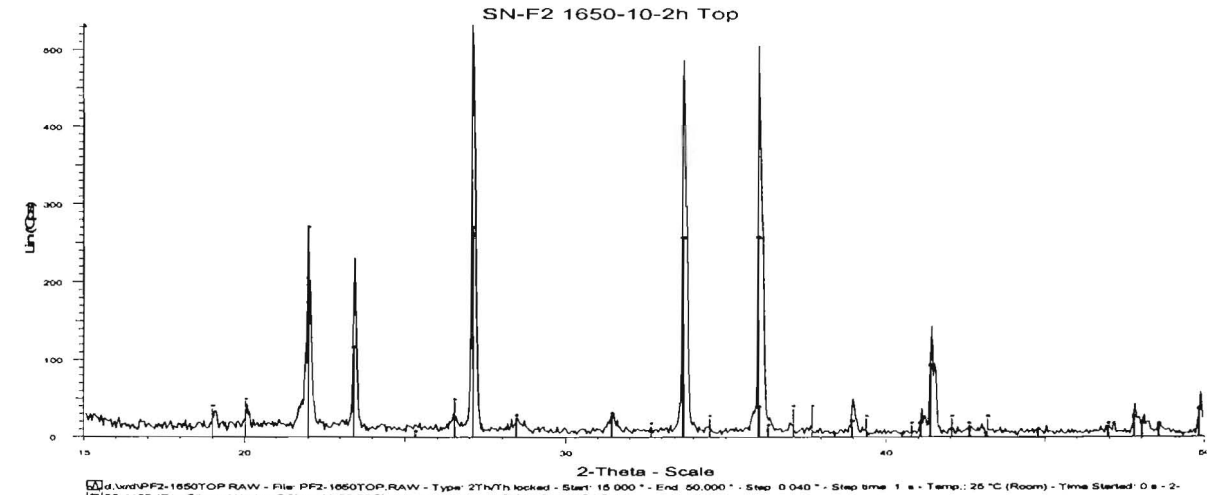

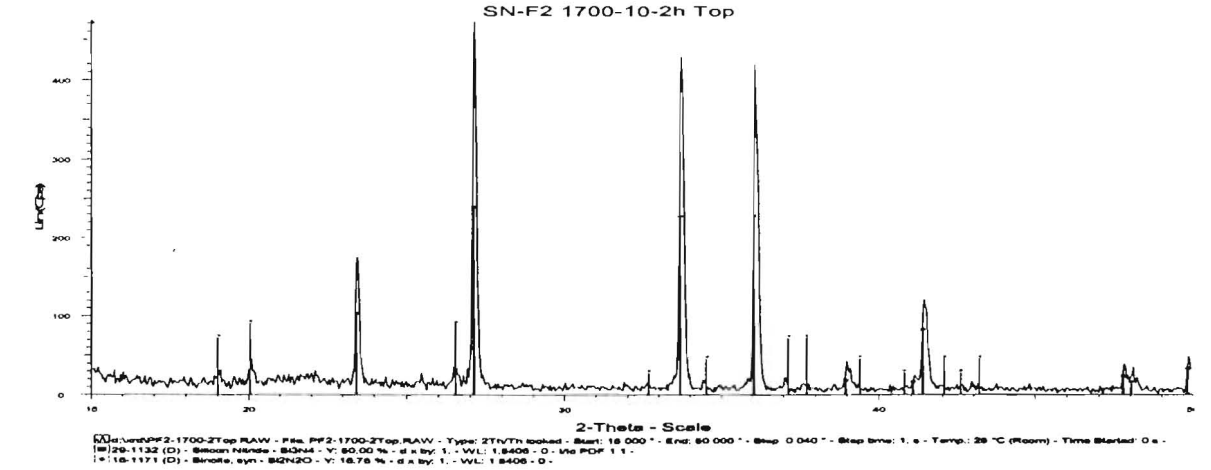

Fig. A-1 Example of XRD patterns of specimens and packing powders after sintering

APPENDIX 2

Table A-2a Results of fracture toughness (K_{IC}) and Vickers hardness (Hv) of sintered specimens at 1700 ^{o}C. (Crack length was measured by SEM)

Conditions (Soaking time)	Sample No. (Piece)	c (μm)	A (μm)	K_{IC} (MPa .$m^{1/2}$)	Hv (GPa)
1 h	1	95.60	51.45	4.90	17.16
	2	88.20	52.95	5.18	16.22
	3	126.50	50.00	4.33	18.18
	4	120.60	50.00	4.40	18.18
	5	123.50	51.45	4.50	17.16
Average				4.66	17.38
2 h	1	102.90	54.40	5.05	15.35
	2	97.10	54.40	5.15	15.35
	3	97.10	52.95	5.01	16.24
	4	105.90	52.95	4.87	16.24
	5	102.90	52.95	4.91	16.24
Average				5.00	15.88

Table A-2b Results of fracture toughness (K_{IC}) and Vickers hardness (Hv) of sintered specimens at 1700 ^{o}C. (Crack length was measured by Optical microscope, OM)

Conditions (Soaking time)	Sample No. (Piece)	c (μm)	a (μm)	K_{IC} (MPa .$m^{1/2}$)	Hv (GPa)
1 h	1	93.20	51.40	5.29	17.21
	2	102.30	53.50	5.13	15.88
	3	108.90	51.40	5.05	17.21
	4	90.40	52.30	5.40	16.62
	5	105.00	53.50	4.99	15.88
Average				5.17**	16.56*
2 h	1	85.00	54.80	5.47	15.14
	2	93.70	54.30	4.90	15.42
	3	96.40	53.60	5.07	15.82
	4	96.20	52.90	5.24	16.25
	5	97.40	53.20	5.01	16.06
Average				5.13**	15.74*

Note: Scale 1 mm = 20 μm

** The average fracture toughness (K_{IC}) of both conditions is taken as ~ 5 MPa .$m^{1/2}$ The equation of median crack is applied for the calculation of K_{IC}.

* The average Vickers hardness (Hv) of both conditions is taken as ~ 16 MPa

Table A-2c Calculated results of biaxial bending strength, S

Lot of powder B	Sample No. (Piece)	Diameter, c (mm)	Thickness, d (mm)	P (N)	S (MPa)
Lot 3	1	2.71	1.48	762.00	487.26
	2	2.71	1.48	715.80	457.72
	3	2.71	1.48	791.40	506.06
	4	2.71	1.48	577.20	369.09
	5	2.71	1.48	542.60	346.97
	6	2.73	1.47	678.80	434.06
	7	2.71	1.46	608.10	388.85
Average					427.14*
Lot 4	1	2.73	1.44	621.20	397.23
	2	2.71	1.48	740.20	473.32
	3	2.71	1.48	582.90	372.74
	4	2.73	1.51	391.00	250.03
	5	2.71	1.49	730.50	467.12
	6	2.71	1.50	684.00	437.38
	7	2.70	1.49	530.60	339.29
Average					414.51*

* The average flexural strength of 427.14 and 414.51 MPa = 420.83 MPa

$S = -0.2387\ P\ (X - Y)/d^2$ ----(1)

Where;

S = maximum center tensile stress (MPa),

P = total load causing fracture, (N),

$X = (1+\nu)\ \ln (B/C)^2 + [(1-\nu)/2](B/C)^2$,

$Y = (1+\nu)[1+ \ln (A/C)^2] + (1-\nu)(A/C)^2$

ν = Poisson's ratio, 0.23,

A = radius of support circle (12.5 mm),

B = radius of loaded area or ram tip (2.5 mm),

C = radius of specimen (13.5 mm), and

d = specimen thickness at fracture origin (1.5 mm).

$\ln\ln 1/S = m\ln\sigma - m\ln\sigma_o$ ----(2)

where;

m = Weibull moldulus

σ = Fracture strength

σ_o= Normalizing parameter

S = Survival probability

APPENDIX 3

Properties of TOSHIBA's specimen (standard bar)
1.Chemical composition

Composition (mass %)			
Si_3N_4	Y_2O_3	Al_2O_3	TiO_2
89.5	4.5	5.0	1.0

2. Estimated real density (theoretical density):
   3.31 g/cm^3
   The above value was obtained by calculation, assuming that 1 % of Si_3N_4 is oxygen. Then, the contents of Si_3N_4 and SiO_2 are 87.82 g and 1.67 g, respectively. Densities of SiO_2, Y_2O_3, Al_2O_3, TiO_2 and Si_3N_4 are 2.20, 4.84, 4.00, 4.25 and 3.21 g/cm^3, respectively.

3. Bulk density and relative density
   Measured bulk density was 3.19 g/cm^3. Then, relative density is 96.4 %

4. Vickers' Hardness
   16.0 GPa
   From the values of P and a, the Value of Vickers hardness is calculated using equation:

$$Hv = 1.8554 \, (P/(2a)^2)$$

Where P = Load (Kg)
a = diagonal distance (mm) of the indent

5. Fracture Toughness
   Crack length was measured by optical microscope and K_{IC} was calculated by two equations.

Crack	K_{IC} (MPa.m$^{1/2}$)
Median crack	5.0
Palmqvist crack	5.9

$$K_{IC} = 0.026 \, \{(E^{1/2}.P^{1/2}.a.c^{-3/2}\} \text{ for Median cracks}$$
$$K_{IC} = 0.018 \, Hv(a^{1/2})(E/Hv^{0.4})\{(c/a)-1\}^{-1/2} \text{ for Palmqvist cracks}$$

Where c = crack length (mm)
E = Young's modulus, ~ 280 GPa

6. Flexural strength of the specimen, ~600-700 MPa.

รายงานการวิจัย

เรื่อง

การพัฒนาวัสดุทดแทนกระดูกสำหรับการผ่าตัดกระดูก

Development of Bone-Substituted Bioimplant Materials

ทุนอุดหนุนการวิจัยจากเงินงบประมาณแผ่นดิน
ประจำปีงบประมาณ 2552
คณะแพทยศาสตร์ จุฬาลงกรณ์มหาวิทยาลัย

โดย

สิทธิศักดิ์ หรรษาเวก

มีนาคม 2553